Polymer-fluorinated silica composite hollow fiber membranes for the recovery of biogas dissolved in anaerobic effluent

Sunee Wongchitphimon[a], Wichitpan Rongwong[a], Chong Yang Chuah[b], Rong Wang[a,c,*]
Tae-Hyun Bae[a,b,*]

a. Singapore Membrane Technology Centre, Nangyang Environment and Water Research Institute, Nanyang Technological University, 1 Cleantech Loop, Singapore 637141, Singapore

b. School of Chemical and Biomedical Engineering, Nanyang Technological University, 62 Nanyang Drive, Singapore 637459, Singapore

c. School of Civil and Environmental Engineering, Nanyang Technological University, 50 Nanyang Avenue, Singapore 639798, Singapore

*Corresponding authors:

E-mail address: rwang@ntu.edu.sg (R. Wang) and thbae@ntu.edu.sg (T.-H. Bae).

Key words: Dissolved methane recovery, biogas, anaerobic digestion, membrane contactor, composite hollow fiber membrane

Highlights

- Highly porous hollow fiber substrates were fabricated with Matrimid®.
- Fluorinated silica nanoparticles were anchored on the substrate surfaces.
- The composite membrane showed an excellent CH_4 recovery performance.
- The composite membrane demonstrated long-term stability in a membrane contactor.

Abstract

In this study, polymer-fluorinated silica composite hollow fiber membranes were fabricated and applied to a membrane contactor system for the recovery of methane dissolved in the anaerobic effluent. Such composite membranes allowed us to tailor the physical property such as porosity and mechanical strength and the surface hydrophobicity in separated processes. To develop the composite membranes, porous hollow fiber substrates were first fabricated with Matrimid®, a commercial polyimide. Subsequently, fluorinated silica particles were synthesized and anchored on the substrates via a strong covalent bonding. Due to the high porosity as well as the high hydrophobicity, our membrane showed an outstanding performance for the recovery of CH_4 in the membrane contactor, such that the CH_4 flux reached 2900 mg CH_4/m^2 –h at the liquid velocity of 0.42 m/s at which the liquid phase still controlled the overall mass transfer. The composite membrane prepared in this work also showed a much better performance in the CH_4 recovery than a commercial polypropylene membrane made for degasification of water. In addition, a long-term test with tap water saturated with the model biogas made up of 60:40 CH_4/CO_2 mixture demonstrated that our membrane can be stably operated for more than 300 hours without experiencing pore wetting problem.

1. Introduction

Anaerobic digestion is a biological process for wastewater treatment which uses microorganism to break down organic pollutants in the absence of oxygen, thereby producing biogas that contains methane, CH_4, as the major component. Since such biogas can be served as an energy source, a self-sufficient wastewater treatment process can potentially be realized if the recovery process is implemented [1]. Meanwhile, both the United States Environmental Protection Agency (EPA) and the Intergovernmental Panel on Climate Change (IPCC) have classified CH_4 as the second most prevalent greenhouse gas since it has 25 times higher global warming potential than that of CO_2 [1]. Therefore, the recovery of CH_4 from anaerobic processes can also be a solution for controlling greenhouse emission to the atmosphere.

Although biogas recovery process from the head spaces of anaerobic reactors has been well established thus far, a significant amount of CH_4 is still dissolved in the anaerobic effluents and is currently discharged without recovery processes. For example, the portion of CH_4 dissolved in the effluent could be as high as 45% when the anaerobic reactor is operated at 30 °C and 1 atm, and this value can further increase at lower temperature [2]. In addition, to prevent any potential explosion problem, the concentration of CH_4 in the effluent must be decreased to the lower explosive limit (LEL) which is reported to be 1.4 mg/l at 15 °C and 1 bar [3]. Thus, the recovery of dissolved CH_4 can not only maximize the overall energy production capacity but also resolve the safety concern associated with potential explosion.

Multi-stage bubble column cross-flow cascades and forced draft aerators have been employed to remove dissolved CH_4 from contaminated water [4]. However, a large mass transfer unit allowing a long residence time is required to achieve 90% dissolved CH_4 removal owing to the poor mass transfer efficiency [5]. To address this issue, membrane-based technology such as membrane contactor has been proposed as a promising alternative [6]. Membrane contactor is a technology that can achieve gas/liquid or liquid/liquid mass transfer without dispersion of one phase within another. Thus, hydrophobic membranes which act as a barrier to separate gas-liquid or liquid-liquid streams are the key element in this technology. It can overcome the limitations of conventional contactors, such as flooding, foaming and high operating cost [7]. The absorption in which the targeted gas is transported from gas phase to liquid sorbent through membrane has been the most popular application for membrane contactor [8-12]. It can also be used in gas desorption application such as, the regeneration of chemical absorbent [13-15]. In this operation, gases physically or chemically trapped in the liquid are desorbed and transferred to the gas phase driven by partial pressure difference which is created by either sweeping gas or vacuum in the gas phase. It has been reported that hollow fiber membrane contactor can effectively perform the gas desorption at a far lower gas-to-liquid ratio than that used in the bubble column [16].

Nevertheless, a limited number of studies on the membrane-based recovery of dissolved CH_4 has been reported thus far [1]. In early studies, nonporous hollow fiber membranes have been employed in membrane contactors which were operated with vacuum [17] or sweeping gas [4] to create a driving force for CH_4 transport. However, unsatisfactory results were observed owing to the high mass transfer resistances of nonporous membranes. An improved performance was observed when microporous membrane was employed [18]. In particular, it was reported that the

CH_4 recovery efficiency of microporous membrane could be 93% higher than that of nonporous membrane at a low liquid velocity. However, in the same work, a drawback of the microporous membranes was also reported as they are prone to the membrane wetting. The membrane wetting is a phenomenon in which water penetrates into membrane pores and cause an extra mass transfer resistance. It typically occurs when the surface hydrophobicity of membrane is not high enough to protect the pores from water. In addition, McLeod et al. [19] reported that the purity of CH_4 in recovered gas increased with an increase in liquid velocity or a decrease in sweeping gas flow rate. Besides, in order to get high purity CH_4, it was recommended to operate with vacuum mode. These significantly increase the transmembrane pressure and may cause the undesirable pore wetting.

All previous studies which were conducted with commercial membranes demonstrated that it is desirable for membrane to possess a high porosity together with a high hydrophobicity for this application. Such properties allow a high gas flux due to the low mass transfer resistance in membrane as well as a long term membrane stability by preventing the pore wetting problem. Herein, we report polymer-fluorinated silica composite hollow fiber membranes for the efficient recovery of CH_4 from anaerobic effluents. Two porous hollow fiber substrates possessing different morphology were fabricated using Matrimid®, a commercial polyimide, to investigate the effect of morphological property on gas transport performance in membrane contactor. As the polymer doesn't have a sufficient hydrophobicity for membrane contactor application, the surfaces of membranes were then modified by depositing fluorinated silica nanoparticles that can render an excellent hydrophobicity. Subsequently, CH_4 recovery performances of the resulting

membranes were evaluated and benchmarked against a commercial porous membrane. Finally, the long-term stability of membrane in a membrane contactor system was evaluated.

2. Experimental

2.1 Materials

Matrimid® 5218 was purchased from Ciba Specialty Chemicals Performance Polymers and used as the hollow fiber membrane material. *N*-methyl-2-pyrrolidone (NMP, >99.5%, Merck), lithium chloride (LiCl, anhydrous, Merck), polyethylene glycol (PEG, MW 200, Samchun Pure Chemical), (3-aminopropyl) trimethoxysilane (APTMS, 97%, Aldrich), tetraethyl orthosilicate (TEOS, ≥99%, Merck), *1H,1H,2H,2H*-perfluorodecyltriethoxysilane (PFTS, 97%, Aldrich), 2-propanol (IPA, 99.9%, Merck), ammonium hydroxide (26% $NH_3.H_2O$, Merck), ethanol (Merck) and *n*-hexane (96%, Merck) were used for membrane fabrication and modification. All reagents were used as received without further purifications. Purified water by a Milli-Q system (18 M Ω cm) was used as the bore fluid during the hollow fiber spinning.

2.2 Fabrication and surface modification of hollow fiber membranes

Matrimid® and LiCl were dried at 50 °C in a vacuum oven for 1 day to remove moisture prior to dope preparation. Definite amounts of the polymer, additives (PEG and LiCl) and solvent were mixed in a jacket flask equipped with an overhead stirrer and kept at 60 °C which was precisely controlled by a circulator bath. The compositions of polymer dopes (denoted as MT-A and MT-B) are shown in Table 1. After the polymer is completely dissolved, the dope solution was cooled down to room temperature and subsequently degassed under a mild vacuum overnight prior to spinning. Next, porous hollow fiber substrates were fabricated by the dry-jet wet spinning

process using conditions listed in Table 2. In the spinning process, the dope was extruded through a spinneret at a controlled rate and went through a certain air gap before immersing into the coagulation bath. The hollow fibers fabricated were then stored in a water bath for at least 2 days to completely remove residual solvent and additives. Finally, the membranes were immersed in glycerol/water (1:1) mixture to prevent shrinkage during the following drying process at room temperature.

Table 1 Compositions of dope solutions for hollow fiber spinning

Code	Dope composition	
MT-A	Matrimid®/LiCl/NMP	14/4/82
MT-B	Matrimid®/LiCl/PEG-200/NMP	14/2/7/77

Table 2 Hollow fiber spinning conditions

Parameter	Value
Bore fluid (NMP/H_2O) (wt%)	80/20
Bore fluid flow rate (ml/min)	2
Air gap (cm)	5
Take up speed	Free fall
External coagulant	Tap water
Spinning temperature (°C)	25
Spinneret diameter (OD/ID) (mm)	1.5/0.7

To render a hydrophobicity to both MT-A and MT-B substrates, fluorinated silica nanoparticles were formed and anchored on the polyimide membrane surfaces via covalent bonding formed by cyclic imide ring opening reaction. The detailed procedure is described elsewhere [20]. Briefly, the imide group of Matrimid® membrane was reacted with the amino group of the APTMS to form the amide group in the first step. Subsequently, the APTMS-treated Matrimid® membrane was immersed in the SiO_2 precursor (TEOS) solution in which APTMS bound to the membrane surface reacted with TEOS to form SiO_2 nanoparticles. Finally, the membrane with SiO_2 nanoparticles were soaked in a PFTS solution, such that PFTS molecules were opt to react with the silanol groups on SiO_2 particles. Depending on the substrates, the surface modified membranes were denoted as Mo-MT-A and Mo-MT-B, respectively

2.3 Membrane characterizations

The dimensions of hollow fiber membranes were examined using a digital microscope (KEYENCE, VHX-500F). The cross section and the surface morphologies of membranes were observed with Scanning Electron Microscope (SEM, JSM-7200F JOEL) at an operation voltage of 5 kV. Dried membrane samples were cryogenically fractured in liquid nitrogen and then coated with a thin layer of platinum using a JEOL JEC-3000FC sputter coater prior to analysis. The membrane surfaces were also analyzed with Atomic Force Microscope (AFM, NX-10 Park System) allowing the quantification of membrane surface roughness as root mean square (RMS) roughness. Pure water permeability (PWP) of membrane was measured to quantify the effective pore space for mass transport. Testing was carried out in a cross flow filtration setup at a constant pressure of 1 bar with deionized water circulated through the lumen side of hollow fiber. Capillary flow porometer (CFP-1500A, Porous Material Incorporated) was employed to

determine the membrane pore size. The tests were conducted by increasing pressure gradually from 0 to 500 psi while measuring the nitrogen gas flow and pressure drop across the samples. The overall membrane porosity, which defined as pore volume divided by total membrane volume, was calculated using the method based on the density measurement [21] as performed in our previous studies [20, 22]. Dynamic water contact angle was measured using a tensiometer (DCAT11 Dataphysics). A hollow fiber sample was fixed to the sample holder and then experienced a cycle of immersion into and emersion from DI water. The contact angle was calculated by the equipment software using the Wihelmy method. Liquid entry pressure of water (LEPw), which is defined as the minimum pressure at which pure water penetrates into dried membrane pores, was measured using a dead-end hollow fiber module. This value is known to be associated with both pore size and hydrophobicity of membrane [23]. Detailed methodology is described in an earlier work by Smolders and Franken [24].

2.4 Recovery of dissolved methane in membrane contactor

The membrane contactor setup for the recovery of dissolved biogas is depicted in Fig.1. Hollow fiber module was prepared using a Teflon® tube having the inside diameter of 0.68 cm and the effective length of 16 cm. The feed solution which is tap water saturated with model biogas (40:60 CO_2/CH_4, Air Liquide Singapore Private Limited) was prepared in a liquid tank of which temperature and pressure were continuously monitored. The model biogas was continuously supplied during the testing to ensure the saturation of feed water with biogas which was confirmed by monitoring dissolved CH_4 concentration with a methane sensor (Mini-Pro CH_4 sensor, Pro-Oceanus). The CH_4 sensors were calibrated to measure 0-30 mg CH_4/L in aqueous solution with the maximum error of ± 2%. The first CH_4 censor was immersed in the feed tank

and the second one was directly installed in the line of liquid outlet from membrane contactor. Pure nitrogen gas (Air Liquide Singapore Private Limited) was employed as the sweeping gas in this work. Volumetric flow rate and temperature of product gas were automatically recorded by a digital bubble meter (Bios Defender^{TM} 530L) and a data acquisition system. The composition of gas in the permeate side was analyzed by Gas Chromatography (490 Micro GC Biogas Analyzer, Agilent Technologies). The membrane contactor system was operated at room temperature and the data were collected at the steady state.

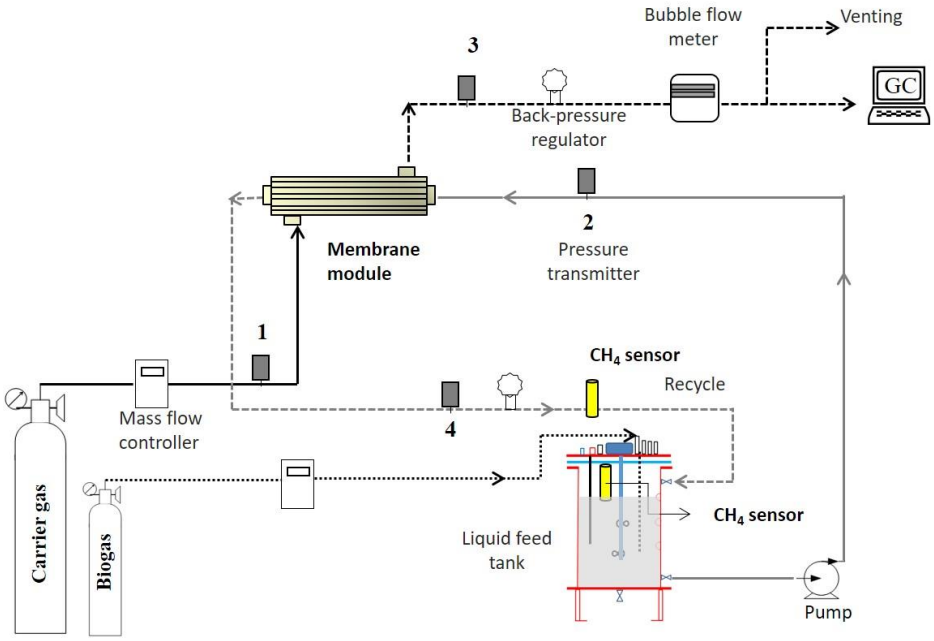

Fig. 1 Membrane contactor system for dissolved CH_4 recovery.

The desorption fluxes and overall mass transfer coefficient of CH_4 and CO_2 (J) were calculated using the following equations:

$$J = \frac{G(Y_{i,out} - Y_{i,in})}{A_T} Mw_i \quad (1)$$

$$K_{OV} = \frac{G(Y_{i,out} - Y_{i,in})}{A_T (C_{i,L} - C^*_{i,G})_{\log mean}} \quad (2)$$

where G is the inert gas flow rate (mol/s), A_T is the mass transfer area calculated from the outer membrane radius (m^2), Mw_i is the molecular weight of CH_4 or CO_2 (mg/mol), Y_{out} and Y_{in} are the mole ratios between CH_4 or CO_2 and the inert gas in the gas phase which can be calculated from the mole fractions of each gas (y_i) as follows:

$$Y_{CH_4} = \frac{y_{CH_4}}{1 - y_{CH_4} - y_{CO_2}} \quad (3)$$

$$Y_{CO_2} = \frac{y_{CO_2}}{1 - y_{CH_4} - y_{CO_2}} \quad (4)$$

The log mean driving force is calculated by the following equations:

$$\left(C_{i,L} - C^*_{i,G}\right)_{\log mean} = \frac{(C_{i,L} - C^*_{i,G})_B - (C_{i,L} - C^*_{i,G})_T}{\ln\left(\frac{(C_{i,L} - C^*_{i,G})_B}{(C_{i,L} - C^*_{i,G})_T}\right)} \quad (5)$$

where $C_{i,L}$ and $C^*_{i,G}$ are the CH_4 or CO_2 concentrations in the liquid phase and equilibrium concentrations in the gas phase, respectively ($kmol/m^3$).). B and T denote bottom (gas outlet) and top (gas inlet) of the membrane module, respectively.

3 Results and discussion

3.1 Porous hollow fiber substrates

To ensure a high flux in membrane contactor operation, membranes should have a high porosity and thereby decrease the mass transfer resistance. Using the conditions described in Table 1 and

2, we could fabricate highly porous hollow fiber substrates of which morphologies are displayed in Fig. 2. Finger-like macrovoids were developed for MT-A for which only LiCl was added to the dope solution, implying an instantaneous solvent-non solvent exchange occurred during the membrane formation. On the other hand, when both PEG and LiCl were added to the dope solution, a significant change in membrane morphology was observed. As shown in Fig. 2b, a sponge-like structure became more prominent in the presence of some large macrovoids. As already demonstrated in the previous studies, the use of mixed additives can effectively slow down the solvent-non solvent exchange, resulting in a formation of interconnected porous structure like sponge [25, 26]. It is noteworthy that the pores formed on our membranes have a circular geometry which may be more beneficial in transporting gas molecules across the membrane than the slit pores typically found in polypropylene and PTFE (polytetrafluoroethylene) membranes.

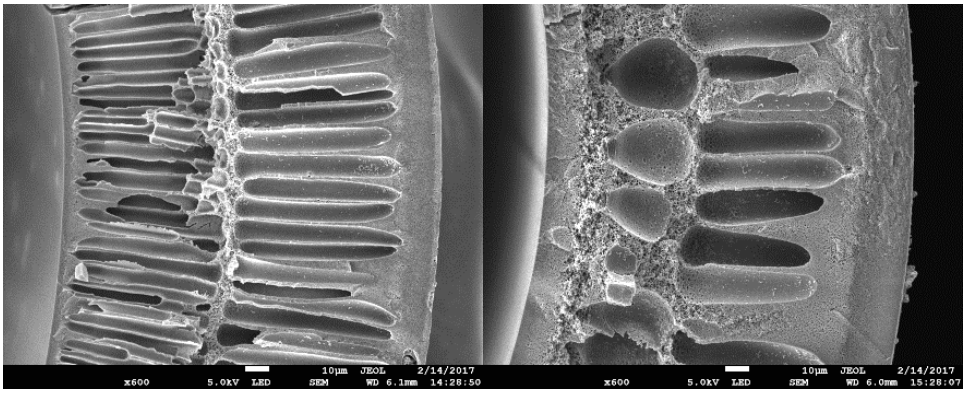

(a) (b)

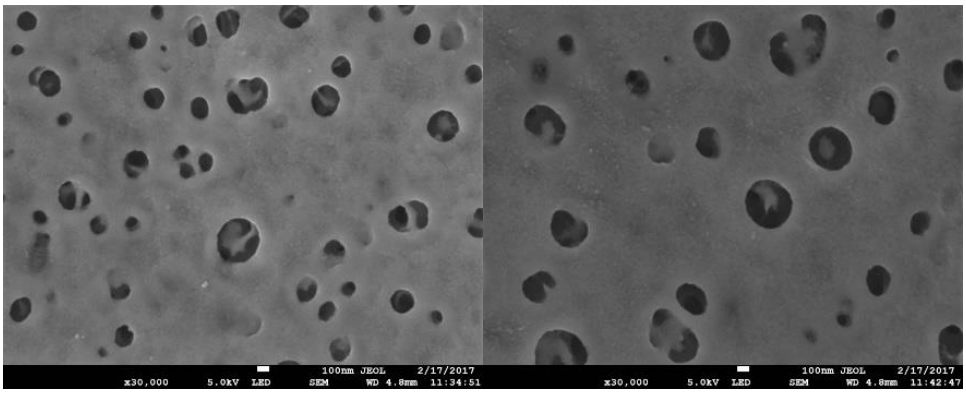

(c) (d)

Fig. 2 SEM images of porous hollow fiber substrates. (a) cross-section of MT-A, (b) cross-section of MT-B, (c) outer surface of MT-A, and (d) outer surface of MT-B

The surfaces of hollow fiber membranes were further analyzed with AFM (Fig. 3). A quantitative analysis showed that MT-A membrane has a higher roughness than MT-B membrane for both outer and inner surfaces (Table 3). However, the difference in surface roughness was too small to cause a significant variance in the water contact angles. The pore analysis revealed that the mean pore sizes of membranes were 55 and 47 nm for MT-A and MT-B, respectively. However, a slightly higher pure water permeability was observed for MT-B, presumably due to the higher porosity which is verified in the next section.

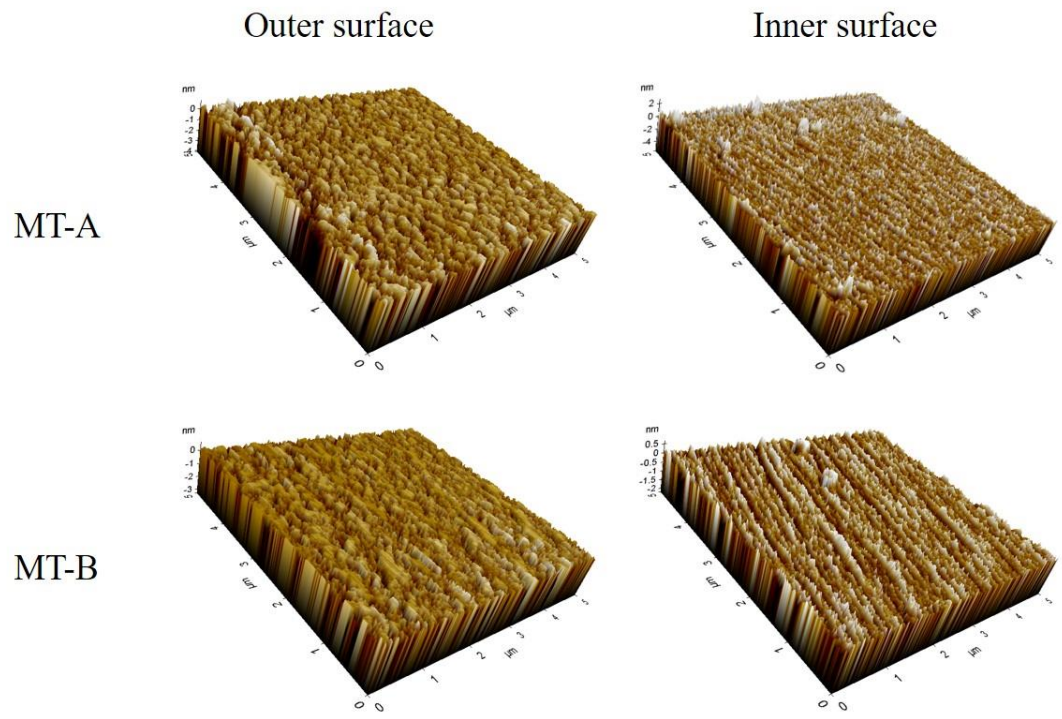

Fig. 3 AFM topographic images of hollow fiber substrates.

Table 3 Characteristics of hollow fiber substrates

Properties	MT-A	MT-B
PWP (kg/m^2 bar h)	179 ± 17	208 ± 15
Mean pore size (nm)	54.8 ± 3.9	46.5 ± 4.2
Water contact angle (°)	75.4 ± 1.3	74.1 ± 0.9
RMS roughness (nm)		
- Outer surface	0.37 ± 0.05	0.32 ± 0.03
- Inner surface	0.39 ± 0.01	0.15 ± 0.03

3.2 Polymer-fluorinated silica composite hollow fiber membranes

In addition to the high porosity, membrane should possess a sufficiently high hydrophobicity to prevent the pore wetting problem that gives rise to a significant decrease in gas flux in membrane contactor. Thus, the porous hollow fiber substrates were hydrophobized using the method we previously developed to fabricate polyetherimide membranes for CO_2 absorption. The detailed reaction mechanism for the formation of fluorinated silica nanoparticles on the polyimide membrane surface is illustrated in the previous work [20, 22]. Successful formation of silica nanoparticles was visually confirmed by SEM as shown in Fig. 4. The amounts of silica nanoparticles formed on membrane surfaces were estimated by thermogravimetric analyzer (TGA). As Matrimid® decomposes completely above 600 °C, the residual mass at 900 °C is from the SiO_2 nanoparticles (TGA curves are now shown). Using the dimensions of hollow fibers (Table 4), the density of Matrimid (1.238 mg/cm^3), and the porosity of membrane (Table 4), the amounts of SiO_2 on Mo-MT-A and Mo-MT-B were calculated to be 2.7 and 2.6 g SiO_2/m^2, respectively. The mass of perfluoro groups on the silica surfaces was neglected in this calculation.

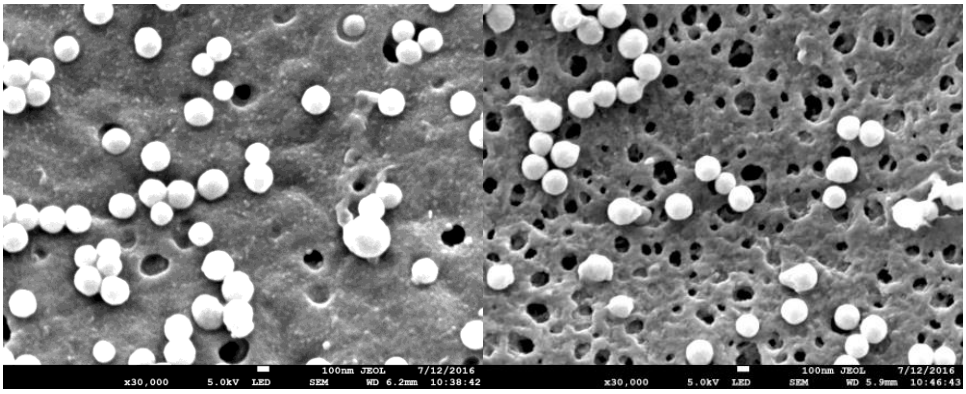

(a) (b)

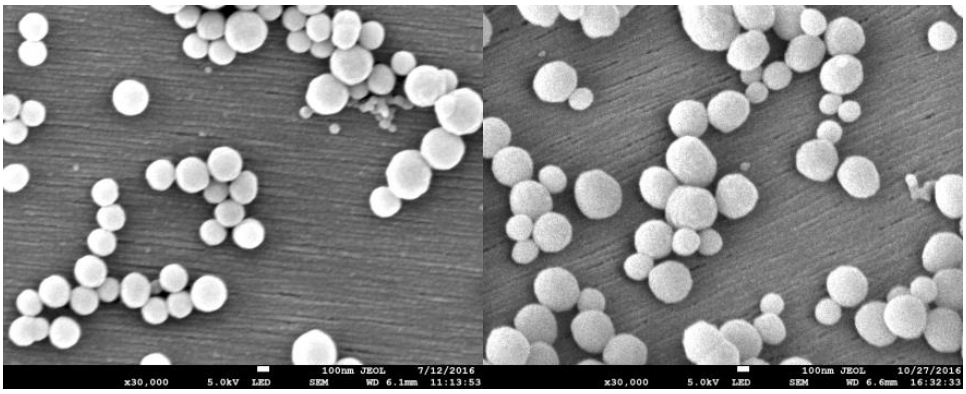

(c) (d)

Fig. 4 SEM images of Matrimid®-fluorinated silica composite hollow fiber membranes. Outer surfaces of (a) Mo-MT-A and (b) Mo-MT-B; inner surfaces of (c) Mo-MT-A and (d) Mo-MT-B

The properties of Matrimid®-fluorinated silica composite membranes are summarized in Table 4. Both MT-A and MT-B membranes showed a significant increase in water contact angle from 75° to 123°, owing to the hydrophobic nature of perfluoro groups on the surface and the change in surface roughness of silica particles. It is noteworthy the water contact angles of our membranes are greater than those of other hydrophobic membranes including PVC, PVDF, PP and PDMS that have been used in membrane contactor applications [27-29]. Due to the increase in hydrophobicity, LEPw of both membranes were observed to be very high in contrast to the original membranes of which the pores are easily accessible by water even at low pressure. Mo-MT-B membrane showed a higher LEPw than Mo-MT-A membrane that possesses larger pores. An analysis on porosity revealed that Mo-MT-B possessing a sponge-like structure has a higher porosity than Mo-MT-A membrane which has finger-like macrovoids.

Table 4 Characteristics of Matrimid®-fluorinated silica composite membranes

Membrane property	Mo-MT-A	Mo-MT-B
Outer diameter (μm)	982 ± 8	983 ± 4
Inner diameter (μm)	675 ± 2	689 ± 4
Thickness (μm)	153 ± 4	147 ± 1
Porosity (%)	59.8 ± 4.7	62.9 ± 2.0
Contact angle (°)	123.8 ± 2.1	122.6 ± 1.8
LEPw (psi)	29.8 ± 3.4	36.2 ± 4.0

3.3 Dissolved CH_4 recovery in the membrane contactor

The hollow fiber membranes prepared were tested for the recovery of CH_4 from the model anaerobic effluent using the system described in Fig.1. In this study, the liquid is fed to the lumen side while the sweeping gas supplied to the shell side of the membrane module in a counter-flow manner. Note that this configuration was reported to be effective in achieving a high CH_4 flux as well as controlling CH_4 loss [30]. We found that the effect of sweeping gas flow rate on CH_4 flux is negligible as the mass transfer resistance at gas phase boundary layer is negligible. This observation is consistent with the previous reports [4, 18]. The theoretical minimum gas to liquid ratio required to separate dissolved CH_4 from the water saturated with biogas is reported to be 0.032 [5]. However, the gas to liquid ratio is recommended to be 3.5 times higher than the minimum to prevent gas phase controlled operation. In the preliminary experiment, the sweeping gas flow rates were varied from 10 to 20 ml/min, which corresponds to the gas to liquid ratio of 0.17-0.80. Under these conditions, we found that the effect of sweeping gas flow rate on CH_4

flux is negligible as the mass transfer resistance at gas phase boundary layer is negligible as compared to the resistance of liquid phase boundary layer. Therefore, the sweeping gas flow rate was fixed at 20 ml/min in all experiments later in this work.

Fig. 5a shows CH_4 fluxes of two different membranes at various liquid velocities. The CH_4 flux gradually increased with an increase in the liquid velocity for both membranes due to a decrease in liquid boundary layer resistance [19]. This is further confirmed by the mass transfer analysis. As shown in Fig 5c, the overall mass transfer coefficients almost linearly increased with the liquid velocity. This observation which is known to be a typical behavior for solutes with small Henry's law constants in the membrane contactors indicates that the mass transfer resistance at liquid boundary layer plays a critical role in the transport of CH_4 in hollow fiber membrane contactor [4, 18, 19]. Meanwhile, Mo-MT-B membrane with sponge-like morphology showed higher CH_4 fluxes (1900 - 2900 mg CH_4/m^2-h) than those of Mo-MT-A membrane (1700 – 2700 mg CH_4/m^2-h) having finger-like macrovoids presumably due to the higher porosity and LEPw. In addition, the membranes could also desorb CO_2 dissolved in the model anaerobic effluent as shown in Fig. 5b. Since much larger amount of CO_2 can be dissolved in the feed solution than CH_4 due to its high solubility, CO_2 fluxes were observed to be higher than those of CH_4 for both membranes. This result implies that further purifications are required as in biogas upgrading processes if the goal is injecting into natural gas grid.

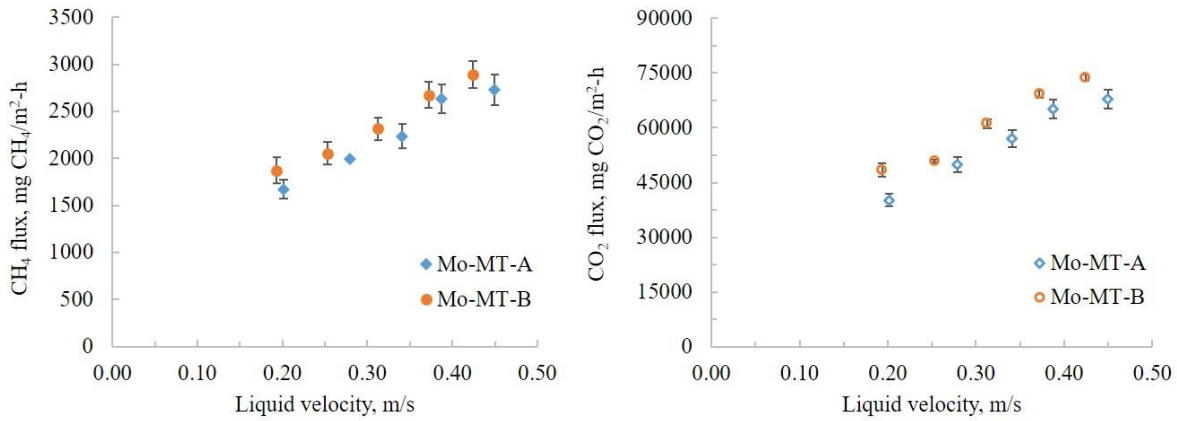

(a) (b)

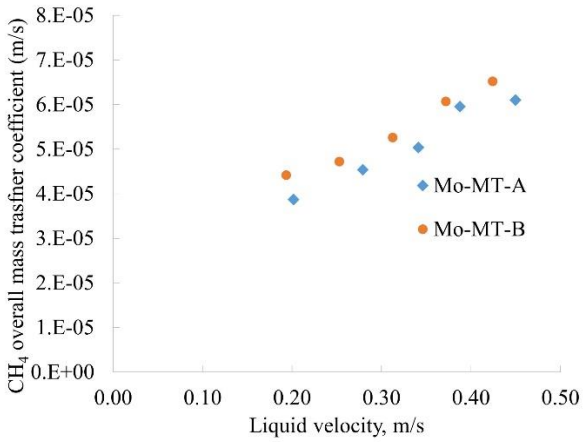

(c)

Fig. 5 (a) CH_4 and (b) CO_2 permeation fluxes of Matrimid®-fluorinated silica composite membranes at various liquid velocities. (c) Overall mass transfer coefficient of CH_4 desorption from Mo-MT-A and Mo-MT-B membranes.

3.4 Comparative study with a commercial membrane

Our membrane (Mo-MT-B) was benchmarked against a commercial polypropylene (PP) (Edgecross-ETC membrane, Suzhou Edgecross Membrane Technology Co., Ltd.) microporous hollow fiber membrane which is designed for removal of gas from water (degassing). Our

analysis on this commercial membrane revealed that the thickness, the outer diameter and the mean pore size are 58 μm, 296 μm, and 61 nm, respectively. SEM images of the PP membrane are shown in Fig. 6. The characteristics of membrane modules are summarized in Table 5. Apparently, the PP membrane has a denser structure than Mo-MT-B membrane as evidenced in SEM images (Fig. 6). The CH_4 recovery performances of Mo-MT-B and PP membranes are shown Fig. 7. Owing to the restriction by a small inner diameter of the PP membrane, the tests were carried out at a low liquid velocity range for both membranes. It was found that our Mo-MT-B membrane showed much higher CH_4 fluxes than that of PP membrane. Therefore, in the membrane contactor process for CH_4 recovery from anaerobic effluents, our membrane can provide several potential advantages over the commercial membrane for degassing, such as a higher processing rate, a lower energy consumption for membrane contactor operation, and a higher rate of CH_4 recovery.

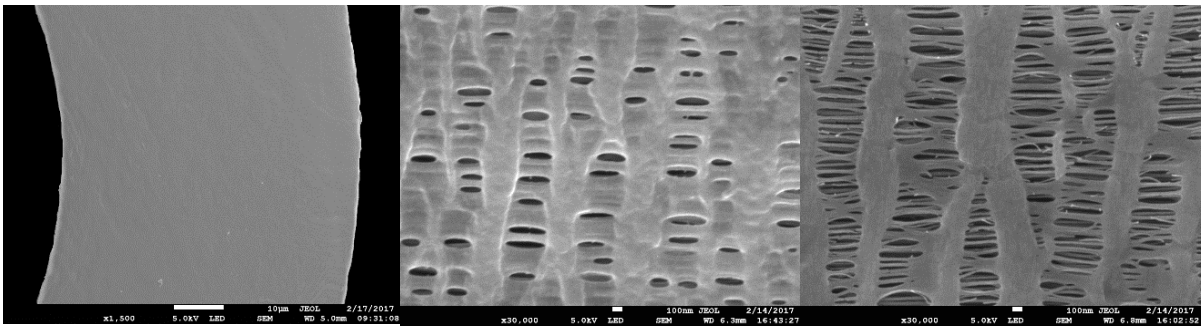

(a) (b) (c)

Fig. 6 SEM images of commercial polypropylene (PP) membrane. (a)cross-section, (b) outer surface, and (c) inner surface

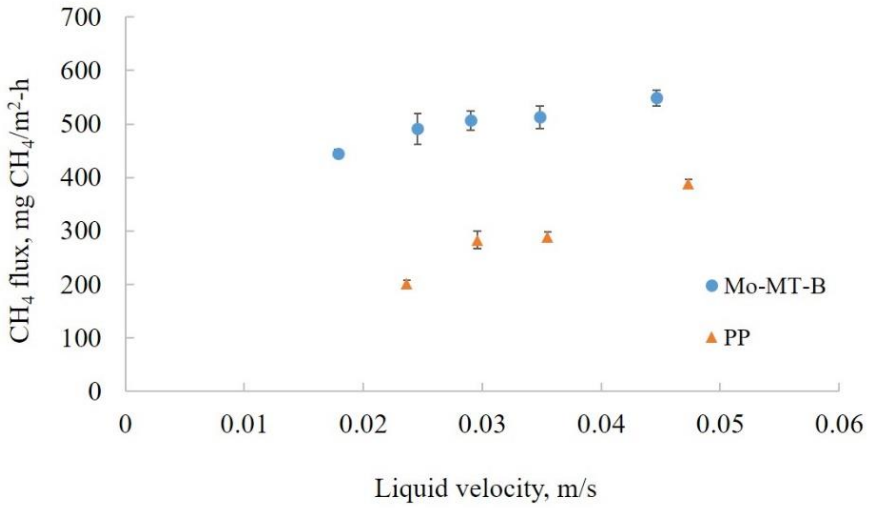

Fig. 7 CH_4 fluxes of Mo-MT-B and commercial PP membranes at various liquid velocities.

Table 5 Characteristics of membrane modules

Parameters	Mo-Mt-A and Mo-Mt-B	PP
Number of fiber	10	111
Membrane length (m)	0.16	
Membrane module (m)	6.8×10^{-3}	
Membrane area (m^2)	4.94×10^{-4}	1.56×10^{-2}
		o.d. 2.96×10^{-4} m
		i.d. 1.80×10^{-4} m
Gas per liquid flow rate ratio	2.5-5	2-5

3.5 Mass transfer analysis

The mass transfer resistances of membranes prepared in this work were determined using the Wilson plot method. Subsequently, the obtained mass transfer resistances from this work were benchmarked against literature data. In this analysis, CO_2 was selected as the transporting component instead of CH_4 because many degassing membranes have been applied to membrane

contactor systems for CO_2 capture and desorption whilst the mass transfer analysis was not conducted in most of CH_4 desorption studies so far. Fig. 8 depicts the Wilson plot of 1/Kol versus $v^{-\propto}$. The α value of 0.7 was found to provide the best linear fit to our experimental data with R^2 values greater than 0.99. The straight line equations and the membrane mass transfer coefficients obtained from their y-intercepts are summarized in Table 6. The membrane mass transfer coefficient of Mo-MT-B which has a highly porous sponge structure is slightly higher than that of Mo-MT-A which was less porous than Mo-MT-B.

Table 7 compares the overall and the membrane mass transfer resistances of our membranes with literature data. The liquid velocities were identical at 0.25 m/s for all membranes except for polyethersulfone membrane which was operated at 0.3 m/s. For all membranes, the overall mass transfer was controlled by liquid phase and therefore the contributions of membrane resistances were ranged in 18-40%. However, the percentage contributions of the membrane resistance were found to be the lowest for our membranes. This is presumably due to the high hydrophobicity of Mo-MT-A and Mo-Mt-B that can prevent the partial membrane wetting. Although PVDF and PP membranes are well known to be hydrophobic, several studies have reported that they can be partially wetted by water due to the capillary condensation of water in membrane pores. This may be attributed to both insufficient hydrophobicity and a broad pore size distribution allowing water to seep into some large pores [31, 32]. Note that our membranes exhibited higher water contact angles (123-125°) than PVDF (92-100°) [33, 34] and PP membranes (100-118°) [35-37] , thereby potentially preventing accumulation of water vapor in pore surface leading to the capillary condensation.

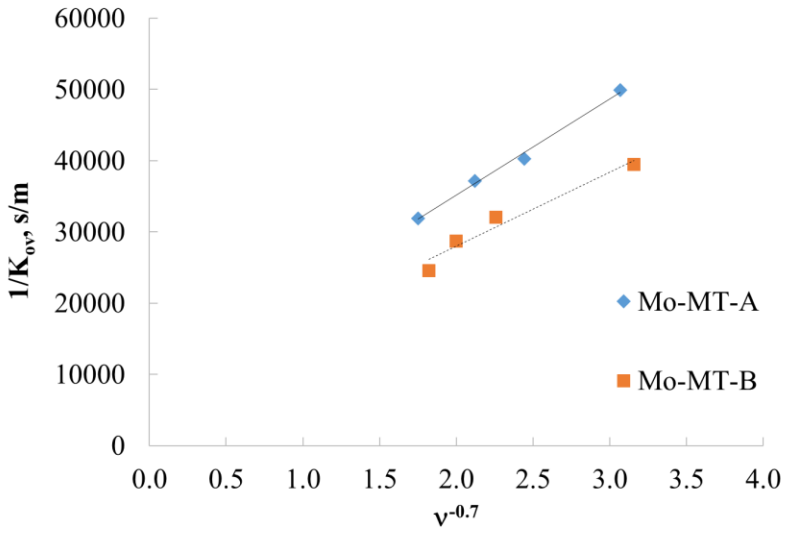

Fig. 8 Wilson plot of Mo-MT-A and Mo-MT-B hollow fiber membrane. CO_2 fluxes were used for the analysis.

Table 6 Wilson plot equations and membrane mass transfer coefficient analysis

Membranes	Equations	R^2	$K_{m,CO2}$ (m/s)
Mo-MT-A	$1/K_{OV,CO2} = 13510v^{-0.7} + 8144.7$	0.994	1.26×10^{-4}
Mo-MT-B	$1/K_{OV,CO2} = 10354v^{-0.7} + 7311.3$	0.96	1.41×10^{-4}

Table 7 Analysis on mass transfer resistances using CO_2 desorption data; the resistances were calculated at the liquid velocity of 0.25 m/s except for PES membrane which was at 0.3 m/s.

Membranes	Membrane mass transfer resistance R_m (s/m)	Pore size (μm)	R_m/R_{total} (%)	References
Mo-MT-A	8144.7	0.055	20.21	Present work
Mo-MT-B	7311.3	0.047	17.68	
PVDF asymmetric	13565	0.2	28.5	[32]

double skin layers				
PVDF asymmetric single skin layer	7,930	0.02	27.7	
Polypropylene (PP)	4,733	0.04	21.8	[38]
Polyethersulfone (PES)	16043	0.009	39.98	[39]

3.6 The long term operation of membrane

A long-term performance of our Mo-MT-B membrane was also investigated to demonstrate the resistance to pore wetting problem. As our surface modification resulted in heterogeneous coverage of fluorinated particles which may cause localized pore wetting issue over a long term exposure to water, the validation of long term stability is particularly important. As shown in Fig. 9, the membrane was continuously operated in the membrane contactor system for more than 300 hours without showing a decrease in membrane performance at a liquid velocity of 0.4 m/s. The fluctuation of CH_4 flux was observed to be less than 15% when the concentration of CH_4 in the feed solution was varied within 5%. This result strongly suggests that the fluorinated silica nanoparticles on the membrane surfaces are stably bound, such that the membrane can maintain its hydrophobicity for a long time. Note that the feed solution used in this work didn't contain any organics or impurities. So, further validation is necessary with real anaerobic effluents in the future.

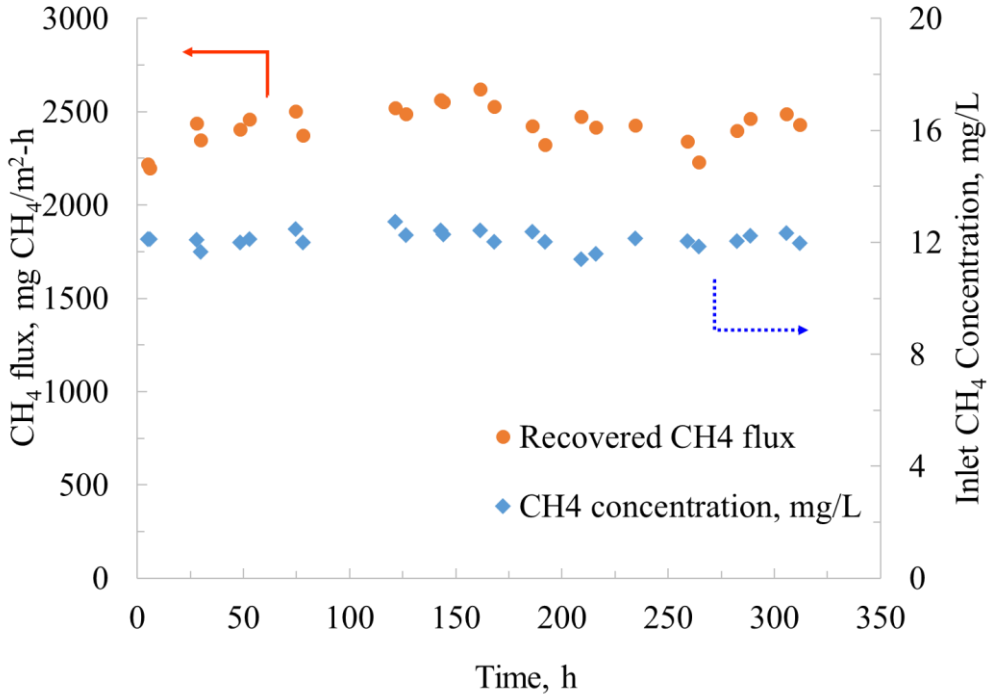

Fig. 9 Long-term performance of Mo-MT-B in the membrane contactor. The feed solution was tab water saturated with the model biogas made up of 60:40 CH_4/CO_2 mixture. The dissolved CH_4 concentration of liquid inlet was maintained at 12–13 mg/L.

4. Conclusions

In this work, we prepared hollow fiber membranes that are specially designed for the recovery of CH_4 dissolved in anaerobic effluents. To realize both a high porosity as well as a high hydrophobicity, the membranes were prepared by two steps: 1) spinning of porous hollow fiber substrates with Matrimid® and 2) deposition of fluorinated silica nanoparticles. Resulting composite membranes showed an excellent CH_4 recovery performance in the membrane contactor that was operated with a model anaerobic effluent. The performance of our membrane also proved to be better than that of commercial PP membrane designed for the degasification of water. Finally, a long-term test revealed that our composite membrane has a good resistance to

pore-wetting that is known to deteriorate the performance of membrane significantly. Future efforts will be devoted to validating the membrane performance with real anaerobic effluents as well as optimizing operation parameters to improve the economic feasibility of membrane contactor system for CH_4 recovery.

Acknowledgments

This research grant is supported by the Singapore National Research Foundation under its Environmental & Water Research Programme (Project Ref No: 1301-IRIS-49) and administered by PUB, Singapore's national water agency. We would also like to thank funding support from the Singapore Economic Development Board to the Singapore Membrane Technology Centre.

References

[1] B.C. Crone, J.L. Garland, G.A. Sorial, L.M. Vane, Significance of dissolved methane in effluents of anaerobically treated low strength wastewater and potential for recovery as an energy product: A review, Water Res., 104 (2016) 520-531.

[2] Z.H. Liu, H. Yin, Z. Dang, Y. Liu, Dissolved Methane: A Hurdle for Anaerobic Treatment of Municipal Wastewater, Environ. Sci. Technol., 48 (2014) 889-890.

[3] A.M. Buswell, T.E. Larson, Methane in ground waters, J. Am. Water Works Assoc., 29 (1937) 1978-1982.

[4] J. Cookney, E. Cartmell, B. Jefferson, E.J. McAdam, Recovery of methane from anaerobic process effluent using poly-di-methyl-siloxane membrane contactors, Water Sci. Technol., 65 (2012) 604-610.

[5] D.W. Hand, J.C. Crittenden, J.L. Gehin, B.W.L. Jr, Design and evaluation of an air-stripping tower fore removing VOCs from groundwater, J. Am. Water Works Assoc., 78 (1986) 87-97.

[6] T.A. Cramer, D.W. Johnson, M.A. Urynowicz, Membrane gas transfer of methane and carbon dioxide in submerged coal deposits, Environ. Technol., 30 (2009) 11-20.

[7] A. Gabelman, S.T. Hwang, Hollow fiber membrane contactors, J. Membr. Sci., 159 (1999) 61-106.

[8] Y. Zhang, R. Wang, Gas–liquid membrane contactors for acid gas removal: recent advances and future challenges, Curr. Opin. Chem. Eng., 2 (2013) 255-262.

[9] Y. Zhang, J. Sunarso, S. Liu, R. Wang, Current status and development of membranes for CO_2/CH_4 separation: A review, Int. J. of Greenh. Gas Control, 12 (2013) 84-107.

[10] S. Masoumi, M.R. Rahimpour, M. Mehdipour, Removal of carbon dioxide by aqueous amino acid salts using hollow fiber membrane contactors, J. CO_2 Util., 16 (2016) 42-49.

[11] J.L. Li, B.H. Chen, Review of CO_2 absorption using chemical solvents in hollow fiber membrane contactors, Sep. Purif. Technol., 41 (2005) 109-122.

[12] Z. Cui, D. deMontigny, Part 7: A review of CO_2 capture using hollow fiber membrane contactors, Carbon Manag., 4 (2013) 69-89.

[13] P. Kosaraju, A.S. Kovvali, A. Korikov, K.K. Sirkar, Hollow Fiber Membrane Contactor Based CO2 Absorption−Stripping Using Novel Solvents and Membranes, Ind. Eng. Chem. Res., 44 (2005) 1250-1258.

[14] N.A. Rahim, N. Ghasem, M. Al-Marzouqi, Stripping of CO_2 from different aqueous solvents using PVDF hollow fiber membrane contacting process, J. Nat. Gas Sci. Eng., 21 (2014) 886-893.

[15] S. Khaisri, D. deMontigny, P. Tontiwachwuthikul, R. Jiraratananon, CO_2 stripping from monoethanolamine using a membrane contactor, J. Membr. Sci., 376 (2011) 110-118.

[16] J. He, R.G. Arnold, A.E. Sáez, E.A. Betterton, W.P. Ela, Removal of Aqueous Phase Trichloroethylene Using Membrane Air Stripping Contactors, J. Environ. Eng., 130 (2004) 1232-1241.

[17] W.M. Bandara, H. Satoh, M. Sasakawa, Y. Nakahara, M. Takahashi, S. Okabe, Removal of residual dissolved methane gas in an upflow anaerobic sludge blanket reactor treating low-strength wastewater at low temperature with degassing membrane, Water Res., 45 (2011) 3533-3540.

[18] J. Cookney, A. McLeod, V. Mathioudakis, P. Ncube, A. Soares, B. Jefferson, E.J. McAdam, Dissolved methane recovery from anaerobic effluents using hollow fibre membrane contactors, J. Membr. Sci., 502 (2016) 141-150.

[19] A. McLeod, B. Jefferson, E.J. McAdam, Toward gas-phase controlled mass transfer in micro-porous membrane contactors for recovery and concentration of dissolved methane in the gas phase, J. Membr. Sci., 510 (2016) 466-471.

[20] Y. Zhang, R. Wang, Novel method for incorporating hydrophobic silica nanoparticles on polyetherimide hollow fiber membranes for CO_2 absorption in a gas–liquid membrane contactor, J. Membr. Sci., 452 (2014) 379-389.

[21] J. Xu, Z.L. Xu, Poly(vinyl chloride) (PVC) hollow fiber ultrafiltration membranes prepared from PVC/additives/solvent, J. Membr. Sci., 208 (2002) 203-212.

[22] Y. Zhang, R. Wang, Fabrication of novel polyetherimide-fluorinated silica organic–inorganic composite hollow fiber membranes intended for membrane contactor application, J. Membr. Sci., 443 (2013) 170-180.

[23] M. Khayet, G. Chowdhury, T. Matsuura, Surface modification of polyvinylidene fluoride pervaporation membranes, AIChE J., 48 (2002) 2833-2843.

[24] K. Smolders, A.C.M. Franken, Terminology for Membrane Distillation, Desalination, 72 (1989) 249-262.

[25] L. Shi, R. Wang, Y. Cao, Effect of the rheology of poly(vinylidene fluoride-co-hexafluropropylene) (PVDF–HFP) dope solutions on the formation of microporous hollow fibers used as membrane contactors, J. Membr. Sci., 344 (2009) 112-122.

[26] S. Wongchitphimon, R. Wang, R. Jiraratananon, L. Shi, C.H. Loh, Effect of polyethylene glycol (PEG) as an additive on the fabrication of polyvinylidene fluoride-co-hexafluropropylene

(PVDF-HFP) asymmetric microporous hollow fiber membranes, J. Membr. Sci., 369 (2011) 329-338.

[27] H. Fashandi, A. Ghodsi, R. Saghafi, M. Zarrebini, CO_2 absorption using gas-liquid membrane contactors made of highly porous poly(vinyl chloride) hollow fiber membranes, International Int. J. of Greenh. Gas Control, 52 (2016) 13-23.

[28] S. Khaisri, D. deMontigny, P. Tontiwachwuthikul, R. Jiraratananon, Comparing membrane resistance and absorption performance of three different membranes in a gas absorption membrane contactor, Sep. Purif. Technol., 65 (2009) 290-297.

[29] S.A. Hashemifard, A.F. Ismail, T. Matsuura, M.R. DashtArzhandi, Performance of silicon rubber coated polyetherimide hollow fibers for CO_2 removal via a membrane contactor, RSC Adv., 5 (2015) 48442-48455.

[30] M. Fang, Z. Wang, S. Yan, Q. Cen, Z. Luo, CO_2 desorption from rich alkanolamine solution by using membrane vacuum regeneration technology, J. of Greenh. Gas Control, 9 (2012) 507-521.

[31] H. Yu, J. Thé, Z. Tan, X. Feng, Modeling SO_2 absorption into water accompanied with reversible reaction in a hollow fiber membrane contactor, Chem. Eng. Sci., 156 (2016) 136-146.

[32] S. Atchariyawut, C. Feng, R. Wang, R. Jiraratananon, D.T. Liang, Effect of membrane structure on mass-transfer in the membrane gas–liquid contacting process using microporous PVDF hollow fibers, J. Membr. Sci., 285 (2006) 272-281.

[33] Y.H. Zhao, Y.L. Qian, B.K. Zhu, Y.Y. Xu, Modification of porous poly(vinylidene fluoride) membrane using amphiphilic polymers with different structures in phase inversion process, J. Membr. Sci., 310 (2008) 567-576.

[34] S. Atchariyawut, R. Jiraratananon, R. Wang, Separation of CO2 from CH4 by using gas–liquid membrane contacting process, J. Membr. Sci., 304 (2007) 163-172.

[35] H. Schönherr, Z. Hruska, G.J. Vancso, Surface Characterization of Oxyfluorinated Isotactic Polypropylene Films: Scanning Force Microscopy with Chemically Modified Probes and Contact Angle Measurements, Macromolecules, 31 (1998) 3679-3685.

[36] V.Y. Dindore, D.W.F. Brilman, F.H. Geuzebroek, G.F. Versteeg, Membrane–solvent selection for CO2 removal using membrane gas–liquid contactors, Sep. Purif. Technol., 40 (2004) 133-145.

[37] C.W. Extrand, A Thermodynamic Model for Wetting Free Energies from Contact Angles, Langmuir, 19 (2003) 646-649.

[38] R. Wang, H.Y. Zhang, P.H.M. Feron, D.T. Liang, Influence of membrane wetting on CO_2 capture in microporous hollow fiber membrane contactors, Sep. Purif. Technol., 46 (2005) 33-40.

[39] G. Bakeri, A.F. Ismail, M. Rahimnejad, T. Matsuura, Porous polyethersulfone hollow fiber membrane in gas–liquid contacting processes, Chem. Eng. Res. Des., 92 (2014) 1381-1390.